

Spin dependent structure function $g_1(x, Q^2)$ at low x and low Q^2

Barbara Badełek ¹

European Organization for Nuclear Research, CERN, Geneva, Switzerland

Dedicated to Jan Kwieciński in honour of his 65th birthday

Abstract: This is a review of experimental and phenomenological investigations of the nucleon spin dependent structure function g_1 at low values of x and Q^2 .

1 Introduction

Spin has for the first time manifested itself experimentally as a new and non-classical quantity in the Stern-Gerlach experiment in 1921, essentially before the birth of the modern quantum mechanics and before (what is being accepted as) the spin discovery. The history of spin, [1], and its predictable future, [2], are both very exciting. With spin research programmes presently operating at BNL, CERN, DESY, JLAB and SLAC and with prospects of polarised $e - p$ collider, EIC, and polarised e^+e^- linear colliders we are witnessing a wide attempt to understand the spin, test the spin sector of QCD and possibly also use it in the search for “new physics”.

This paper is a review of results of the experimental and theoretical investigations of the nucleon spin structure at low values of the Bjorken scaling variable x . This is a region of high parton densities, where new dynamical mechanisms may be revealed and where the knowledge of the spin dependent nucleon structure function $g_1(x, Q^2)$ is

¹On leave of absence from the Institute of Experimental Physics, Warsaw University, Hoża 69, PL-00 681 Warsaw, Poland; e-mail address: badelek@cern.ch

required to evaluate the spin sum rules necessary to understand the origin of the nucleon spin. The behaviour of g_1 at $x \lesssim 0.001$ and in the scaling region, $Q^2 \gtrsim 1 \text{ GeV}^2$, is unknown due to the lack of colliders with polarised beams. Information about spin-averaged structure function $F_2(x, Q^2)$ in that region comes almost entirely from the experiments at HERA: the F_2 rises with decreasing x , in agreement with QCD and the rise is weaker with decreasing Q^2 , [3]. However even if such an inclusive quantity as F_2 can be described by the conventional DGLAP resummation, certain non-inclusive observables seem to be better described by the BFKL approach, [4]. Thus non-inclusive reactions are crucial to understand the dynamics of high parton densities. Unfortunately in the case of spin, the longitudinal structure function, $g_1(x, Q^2)$, is presently the only observable which permits the study of low x spin dependent processes. Since it is being obtained exclusively from fixed-target experiments where low values of x are correlated with low values of Q^2 , one faces new complications: not only the measurements put very high demands on event triggering and reconstruction but also theoretical interpretations of the results require a suitable extrapolation of parton ideas to the low Q^2 region and inclusion of dynamical mechanisms, like the Vector Meson Dominance (VMD). The latter may indeed be important apart of the partonic contributions as it is the case for the low Q^2 spin-averaged electroproduction, see e.g. [5, 6, 7]. In the spin-dependent case and in the $Q^2=0$ limit g_1 should be a finite function of W^2 , free from any kinematical singularities or zeros. For large Q^2 the VMD contribution to g_1 vanishes as $1/Q^4$ and can usually be neglected. The partonic contribution to g_1 which controls the structure functions in the deep inelastic domain and which scales there *modulo* logarithmic corrections, has to be suitably extended to the low Q^2 region.

2 Results of measurements

Experimental knowledge on the longitudinal spin dependent structure function $g_1(x, Q^2)$ comes entirely from the fixed-target setups: EMC, SMC and COMPASS at CERN, experiments at SLAC (E142, E143, E154, E155, E155X) and the HERMES experiment at HERA ep collider. Information on the kinematic variables comes from measurements of the incident and scattered leptons. Hadrons resulting from the target breakup are often also measured, and – in the case of HERMES and COMPASS – identified, if their momenta are larger than 1 GeV in the former- and larger than 2.5 GeV in the latter case.

In fixed-target experiments the low x region is correlated with low values of Q^2 and the range of Q^2 covered at low x is usually limited. In the past the lowest values of x

were reached by the SMC due to a high energy of the muon beam and to a demand of a final state hadron, imposed either in the off-line analysis [8] or in the dedicated low x trigger with a hadron signal in the calorimeter [9]. These requirements permitted measurements of muon scattering angles as low as 1 mrad, Fig.1 and efficiently removed the dominant background of muons scattered elastically from target atomic electrons at $x = 0.000545$, cf. [9]. Much lower values of x are presently being obtained by COMPASS, Fig.2, thanks to a specially designed trigger system, [10]. Charged lepton deep

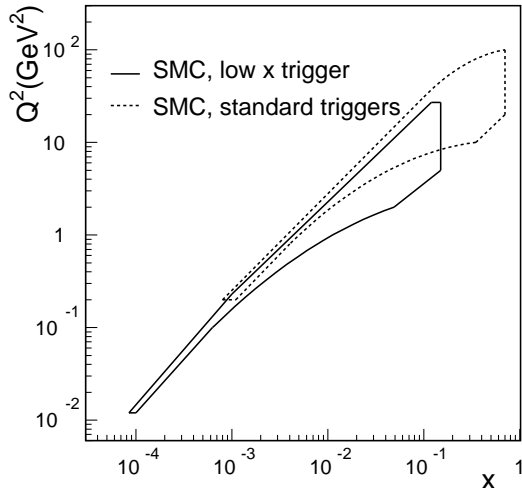


Figure 1: Contours of the kinematic acceptance in the (x, Q^2) plane for the standard triggers (dotted line) and for the low x trigger (solid line) in the SMC. Figure taken from [9].

inelastic scattering experiments benefit from high rates and low (albeit complicated) systematic biases. They have to deal with a strong Q^2 dependence of the cross section (due to photon propagator effects) and with large contribution of radiative processes. Electron and muon measurements are complementary: the former offer very high beam intensities but their kinematic acceptance is limited to low values of Q^2 and moderate values of x , the latter extend to higher Q^2 and to lower values of x (an important aspect in the study of sum rules) but due to limited muon beam intensities the data taking time has to be long to ensure a satisfactory statistics.

Spin-dependent cross sections are only a small contribution to the total deep inelastic cross section. Therefore they can best be determined by measuring the cross section asymmetries in which spin-independent contributions cancel. Direct result of all measurements is thus the longitudinal cross section asymmetry, A_{\parallel} which permits to extract the virtual photon – proton asymmetry, A_1 and finally, using F_2 and R , to get g_1 . Asymmetry A_{\parallel} is small, thus a large statistics is necessary to make a statisti-

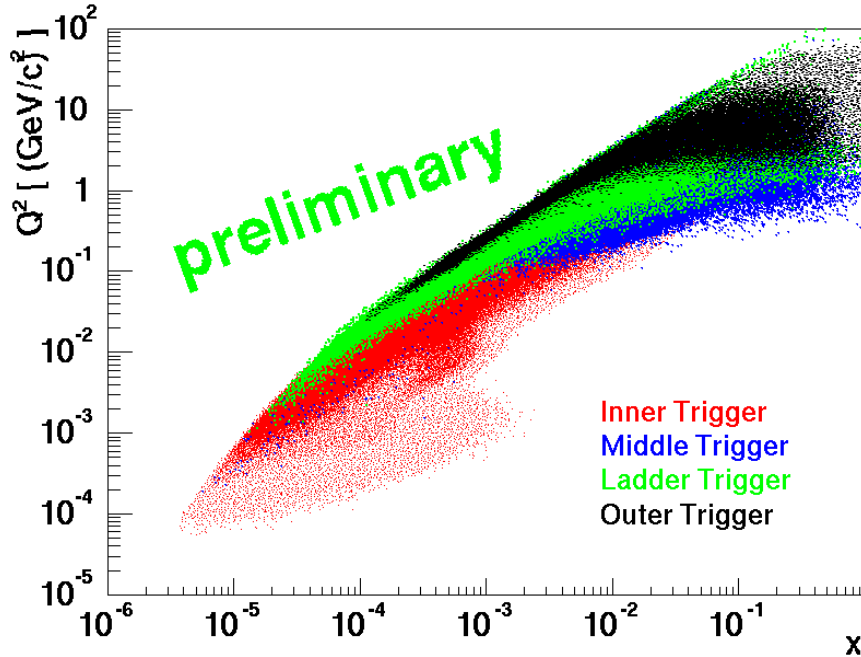


Figure 2: Contours of the kinematic acceptance in the (x, Q^2) plane for the COMPASS triggers. Only about 5% of data taken in 2002 are marked. Figure taken from [10].

cally significant measurement. Problems connected with evaluation of spin structure functions from the data are described in detail in [11].

As a result of a large experimental effort over the years, proton and deuteron g_1 was measured for $0.000\ 06 < x < 0.8$, cf. Fig. 3, [12]. Direct measurements on the neutron are limited to $x \gtrsim 0.02$. No significant spin effects were observed at lowest values of x , explored only by the SMC. Scaling violation in $g_1(x, Q^2)$ is weak: the average Q^2 is about 10 GeV^2 for the SMC and almost an order of magnitude less for the SLAC and HERMES experiments. For the SMC data [9], $\langle x \rangle = 0.0001$ corresponds to $\langle Q^2 \rangle = 0.02\text{ GeV}^2$; Q^2 becomes larger than 1 GeV^2 at $x \gtrsim 0.003$ (at $x \gtrsim 0.03$ for HERMES). At lowest x results on g_1 have very large errors but it seems that both g_1^p and g_1^d are positive there. Statistical errors dominate in that kinematic interval.

3 Regge model predictions

The low x behaviour of g_1 for fixed Q^2 reflects the high energy behaviour of the virtual Compton scattering cross section with centre-of-mass energy squared, $s \equiv W^2 = M^2 + Q^2(1/x - 1)$; here M is the nucleon mass. This is the Regge limit of the (deep) inelastic

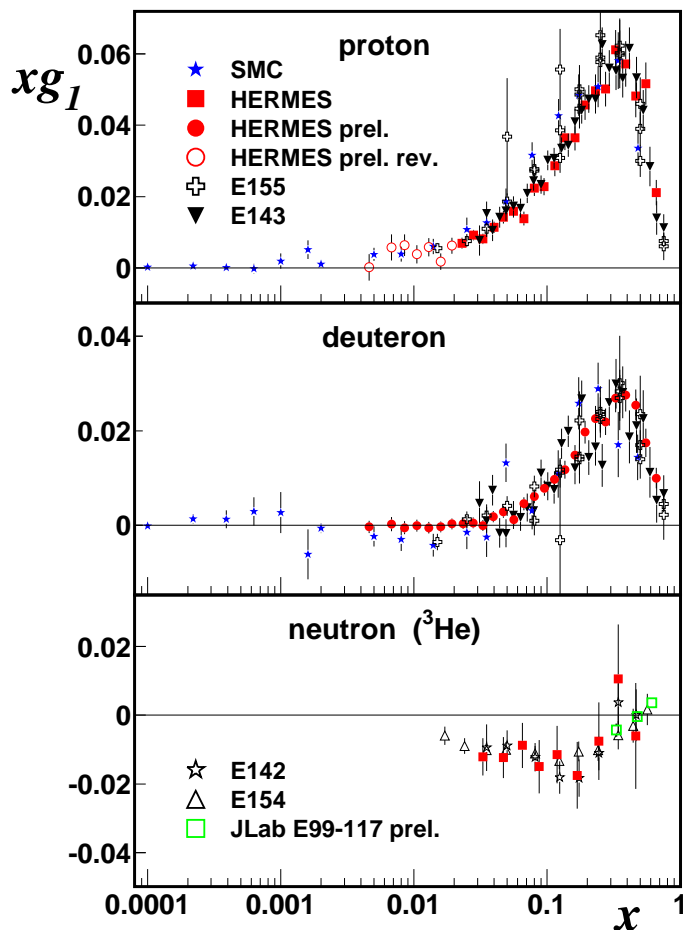


Figure 3: Compilation of data on $xg_1(x, Q^2)$ including new, preliminary data from HERMES and JLAB (E99-117). All the data are given at their quoted mean Q^2 values. Errors are total. Figure taken from [12].

scattering where the Regge pole exchange model should be applicable. This model gives the following parametrisation of the (singlet and nonsinglet) spin dependent structure function at $x \rightarrow 0$ (i.e. $Q^2 \ll W^2$):

$$g_1^i(x, Q^2) \sim \beta(Q^2)x^{-\alpha_i(0)} \quad (1)$$

where the index i refers to singlet (s) and nonsinglet (ns) combinations of proton and neutron structure functions, $g_1^s(x, Q^2) = g_1^p(x, Q^2) + g_1^n(x, Q^2)$ and $g_1^{ns}(x, Q^2) = g_1^p(x, Q^2) - g_1^n(x, Q^2)$ respectively. Intercepts of the Regge trajectories, $\alpha_i(0)$, are universal quantities, independent of the external particles or currents and dependent only on the quantum numbers of the exchanged Regge poles. In the case of g_1 the intercepts correspond to the axial vector mesons with $I=0$ (g_1^s ; f_1 trajectory) and $I=1$ (g_1^{ns} ; a_1 trajectory). It is expected that $\alpha_{s,ns}(0) \lesssim 0$ and that $\alpha_s(0) \approx \alpha_{ns}(0)$, [13]. This behaviour of g_1 should go smoothly to the $W^{2\alpha}$ dependence for $Q^2 \rightarrow 0$. A Regge type

approach has been used in a global analysis of the proton and neutron spin structure function data in the range $0.3 \text{ GeV}^2 < Q^2 < 70 \text{ GeV}^2$ and $4 \text{ GeV}^2 < W^2 < 300 \text{ GeV}^2$, [14]; fits gave a smooth extrapolation of g_1 down to the photoproduction limit.

At large Q^2 it is well known that the Regge behaviour of $g_1(x, Q^2)$ is unstable against the DGLAP evolution and against resummation of the $\ln^2(1/x)$ terms which generate more singular x dependence than that implied by Eq.(1) for $\alpha_{s,ns}(0) \lesssim 0$, cf. Section 4.

Other considerations based on the Regge theory give further isosinglet contributions to the low x behaviour of g_1 : a term proportional to $\ln x$ (from a vector component of the short range exchange potential), [15] and a term proportional to $2 \ln(1/x)-1$ (exchange of two nonperturbative gluons), [16]; a perversly behaving term proportional to $1/(x \ln^2 x)$, recalled in [15] is not valid for g_1 , [17].

Testing the Regge behaviour of g_1 through its x dependence should in principle be possible with the low x data of the SMC [9] which include the kinematic region where W^2 is high, $W^2 \gtrsim 100 \text{ GeV}^2$, and $W^2 \gg Q^2$. Thus the Regge model should be applicable there. However for those data W^2 changes very little: from about 100 GeV^2 at $x = 0.1$ to about 220 GeV^2 at $x = 0.0001$, contrary to a strong change of Q^2 : from about 20 GeV^2 to about 0.01 GeV^2 respectively. Thus those data cannot test the Regge behaviour of g_1 . Moreover employing the Regge model prediction, $g_1 \sim x^0$ to obtain the $x \rightarrow 0$ extrapolation of g_1 , often used in the past to extract the g_1 moments (cf. [18] and Fig.4) is not correct. The values of g_1 should be evolved to a common value of Q^2 before the extrapolation, cf. Eq.(1). Therefore other ways of extrapolation of g_1 to low values of x were adopted in the analyses, see Sections 4.1 and 4.3. Testing the Regge behaviour of g_1 may be possible in COMPASS, cf. Fig. 2.

4 Low x implications from the perturbative QCD

4.1 DGLAP fits to the g_1 measurements

In the standard QCD, the asymptotic, small x behaviour of g_1 is created by the “ladder” processes, Fig.5. In the LO approximation it is given by:

$$g_1(x, Q^2) \sim \exp \left[A \sqrt{\xi(Q^2) \ln(1/x)} \right] \quad (2)$$

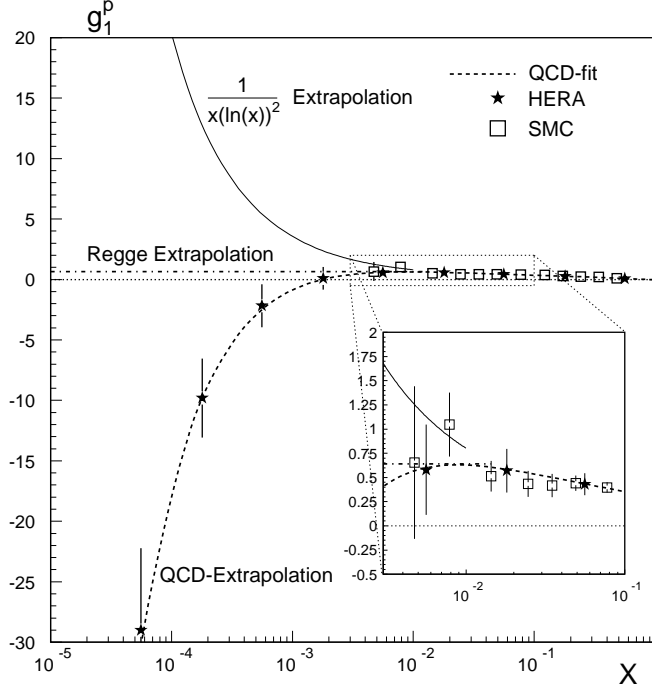


Figure 4: Three scenarios of the possible behaviour of g_1^p at low x [19].

where

$$\xi(Q^2) = \int_{Q_0^2}^{Q^2} \frac{dq^2}{q^2} \frac{\alpha_s(q^2)}{2\pi} \quad (3)$$

and the constant A is different for singlet and non-singlet case. The above behaviour of g_1 is more singular than that implied by Eq.(1) for $\alpha_{s,ns}(0) \lesssim 0$: Regge behaviour of $g_1(x, Q^2)$ is unstable against the QCD evolution. Let us mention for comparison that in the spin-averaged case, $x F_1^s$ has the small x behaviour as that in Eq.2 (in the Regge theory F_1^s is controlled by the exchange of the pomeron with intercept ~ 1.08) while F_1^{ns} remains stable under the QCD evolution (F_1^{ns} is controlled by the exchange of the A_2 trajectory of intercept ~ 0.5).

Several analyses of the Q^2 dependence of g_1 have been performed on the world data [18,21,22,23,24,25], in the framework of the NLO QCD. However the present data do not permit to determine the shapes of parton distributions with sufficient accuracy. This is true especially for the small x behaviour of parton densities where neither the measurements nor the calculations of possible new dynamic effects exist. Thus extrapolations of the DGLAP fit results to the unmeasured low x region give different g_1 behaviours in different analyses, e.g. g_1^p at $x \lesssim 0.001$ is positive and increasing with decreasing x in [25], Fig. 6 and negative and decreasing in [18,22]. It should be

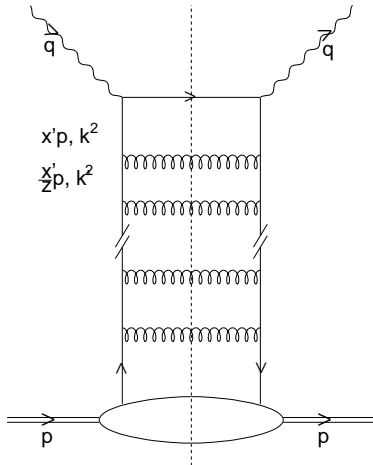


Figure 5: An example of a “ladder” diagram. Figure taken from [20].

stressed that the g_1 results for x values below these of the data do not influence the results of the fit. Thus there is no reason to expect that the partons at very low x behave as those in the measured (larger x) region. Nevertheless extrapolations of the QCD fit are presently being used to get the $x \rightarrow 0$ extrapolation of g_1 [18], necessary to evaluate its first moments. They strongly disagree with the Regge asymptotic form, cf. Fig. 4.

4.2 Double logarithmic $\ln^2(1/x)$ corrections to $g_1(x, Q^2)$

The LO (and NLO) QCD evolution which sums the powers of $\ln(Q^2/Q_0^2)$ is incomplete at low x . Powers of another large logarithm, $\ln(1/x)$, have to be summed up there. In the spin-independent case this is accomplished by the BFKL evolution equation (see e.g. [26]) which gives the leading low x behaviour of the structure function, e.g. $F_1^s \sim x^{-\lambda_{BFKL}}$ where $\lambda_{BFKL} > 1$.

It has recently been pointed out that the small x behaviour of both singlet and non-singlet spin dependent structure function $g_1(x, Q^2)$ is controlled by the double logarithmic terms, i.e. by those terms of the perturbative expansion which correspond to powers of $\alpha_s \ln^2(1/x)$ at each order of the expansion, [27]. The double logarithmic terms also appear in the non-singlet spin averaged structure function F_1^{ns} [28] but the leading small x behaviour of the F_1^{ns} which they generate is overridden by the (non-perturbative) contribution of the A_2 Regge pole, [29]. In case of the g_1 its Regge behaviour is unstable against the resummation of the $\ln^2(1/x)$ terms which generate

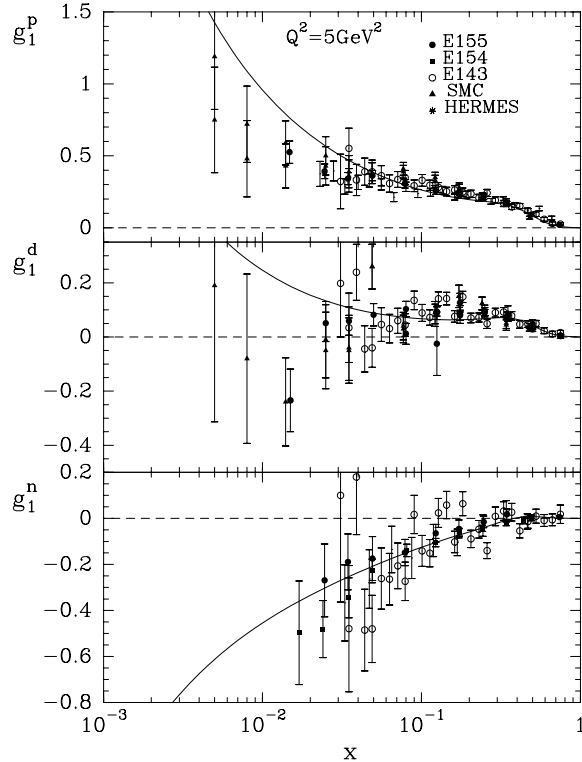


Figure 6: Spin dependent structure functions of proton, deuteron and neutron from a global NLO QCD analysis in a statistical picture of the nucleon at $Q^2 = 5 \text{ GeV}^2$ (curves). The curves maintain their behaviour at least down to $x \sim 10^{-5}$. Figure taken from [25].

more singular x dependence than that implied by Eq.(1) for $\alpha_{s,ns} \lesssim 0$, i.e. they generate the leading small x behaviour of the g_1 .

The double logarithmic terms in the non-singlet part of the $g_1(x, Q^2)$ are generated by ladder diagrams [30, 31] as in Fig. 5. Contribution of non-ladder diagrams [27] in the non-singlet case is non-leading in the large N_c limit (N_c is a number of colours); it is numerically small for $N_c=3$. The contribution of non-ladder diagrams is however non-negligible for the singlet spin dependent structure function; they are obtained from the ladder ones by adding to them soft bremsstrahlung gluons or soft quarks, [32]. At low x , the singlet part, g_1^s dominates g_1^{ns} .

The double logarithmic $\ln^2(1/x)$ effects go beyond the standard LO (and NLO) QCD evolution of spin dependent parton densities. They can be accommodated for in the QCD evolution formalism based upon the renormalisation group equations, [34]. An alternative approach is based on unintegrated spin dependent parton distributions, $f_j(x', k^2)$ ($j = u_v, d_v, \bar{u}, \bar{d}, \bar{s}, g$) where k^2 is the transverse momentum squared of the parton j and x' the longitudinal momentum fraction of the parent nucleon carried by

a parton [20, 32, 33]. This formalism is very suitable for extrapolating g_1 to the region of low Q^2 at fixed W^2 , [20].

The conventional (integrated) distributions $\Delta p_j(x, Q^2)$ (i.e. $\Delta q_u = \Delta p_{u_v} + \Delta p_{\bar{u}}$, $\Delta \bar{q}_u = \Delta p_{\bar{u}}$ etc. for quarks, antiquarks and gluons) are related in the following way to the unintegrated distributions $f_j(x', k^2)$:

$$\Delta p_j(x, Q^2) = \Delta p_j^0(x) + \int_{k_0^2}^{W^2} \frac{dk^2}{k^2} f_j(x' = x(1 + \frac{k^2}{Q^2}), k^2) \quad (4)$$

Here $\Delta p_j^0(x)$ denote the nonperturbative parts of the of the distributions, corresponding to $k^2 < k_0^2$ and the parameter k_0^2 is the infrared cut-off ($k_0^2 \sim 1 \text{ GeV}^2$). In [20, 33, 32] they were treated semiphenomenologically and were parametrised as follows:

$$\Delta p_j^0(x) = C_j(1 - x)^{n_j} \quad (5)$$

The unintegrated distributions $f_j(x', k^2)$ are the solutions of the integral equations [20, 33, 32] which embody both the LO Altarelli-Parisi evolution and the double $\ln^2(1/x')$ resummation at small x' . These equations combined with Eq.(4) and with a standard relation of g_1 to the polarised quark and antiquark distributions Δq_i and $\Delta \bar{q}_i$ corresponding to the quark (antiquark) flavour i :

$$g_1(x, Q^2) = \frac{1}{2} \sum_{i=u,d,s} e_i^2 [\Delta q_i(x, Q^2) + \Delta \bar{q}_i(x, Q^2)]. \quad (6)$$

(assuming $\Delta \bar{q}_u = \Delta \bar{q}_d$ and number of flavours equal 3) lead to approximate $x^{-\lambda}$ behaviour of the g_1 in the $x \rightarrow 0$ limit, with $\lambda \sim 0.4$ and $\lambda \sim 0.8$ for the nonsinglet and singlet parts respectively which is more singular at low x than that generated by the (nonperturbative) Regge pole exchanges.

Results of a complete, unified formalism incorporating the LO Altarelli-Parisi evolution and the $\ln^2(1/x)$ resummation at low x for g_1^p are shown in Figs 7 and 8, separately for the total [32] and nonsinglet [20] parts of the spin dependent structure function. Resummation of $\ln^2(1/x)$ terms gives g_1 steeper than that generated by the LO evolution alone and this effect is in g_1^{ns} visible already for $x \lesssim 10^{-2}$.

The double $\ln^2(1/x)$ effects are not important in the W^2 range of the fixed target experiments. However since $x(1 + k^2/Q^2) \rightarrow k^2/W^2$ for $Q^2 \rightarrow 0$ in the integrand in Eq. (4) and since $k^2 > k_0^2$ there, the $g_1(x, Q^2)$ defined by Eqs (6) and (4) can be smoothly extrapolated to the low Q^2 region, including $Q^2 = 0$. In that limit, the g_1 should be a finite function of W^2 , free from any kinematical singularities or zeros. The extrapolation, valid for fixed and large W^2 , can thus be done provided that nonperturbative parts of the parton distributions $\Delta p_j^0(x)$ are free from kinematical

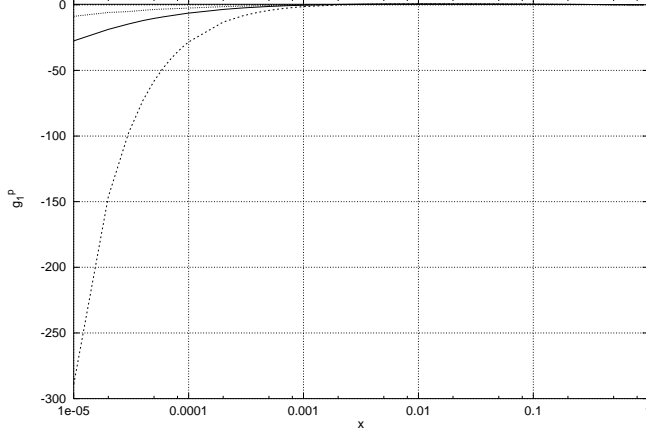


Figure 7: $g_1^p(x, Q^2)$ at $Q^2=10 \text{ GeV}^2$. A thick solid line corresponds to full calculations, a dashed one – only the ladder $\ln^2(1/x)$ resummation with LO Altarelli-Parisi evolution, a dotted one - pure LO Altarelli-Parisi evolution and a thin solid line - the nonperturbative input, $g_1^{(0)}$, related to $\Delta p_j^0(x)$ in Eq.4. Figure taken from [32].

singularities at $x = 0$, as in the parametrisations defined by Eq. (5). If however $\Delta p_j^0(x)$ contain kinematical singularities at $x=0$ then one may replace it with $\Delta p_j^0(\bar{x})$ where $\bar{x} = x(1 + k_0^2/Q^2)$ and leave the remaining parts of the calculations unchanged.

The formalism including the $\ln^2(1/x)$ resummation and the LO Altarelli-Parisi evolution, [32], was used to calculate g_1 at x and Q^2 values of the SMC measurement and a reasonable description of the data on $g_1^{p,d}(x, Q^2)$ extending down to $x \sim 0.0001$ at $Q^2 \sim 0.02 \text{ GeV}^2$ was obtained, cf. Fig.1 in [35]. Of course the (extrapolated) partonic contribution may not be the only one at low Q^2 ; the VMD part may play a non-negligible role as well, cf. Section 5.

4.3 Low x contributions to g_1 moments

Fundamental tools in investigating the properties of the spin interactions are the sum rules, expected to be satisfied by the spin structure functions. These sum rules involve first moments of g_1 , i.e. integrations of g_1 over the whole range of x values, from 0 to 1. This means that experimentally unmeasured regions, $[0, x_{min})$ and $(x_{max}, 1]$ must also be included in the integrations. The latter is not critical, see e.g. [11], but contribution from the former may significantly influence the moments. The value of x_{min} depends on the value of the maximal lepton energy loss, ν_{max} , accessed in an experiment at a given Q_0^2 . For the CERN experiments, with muon beam energies about 200 GeV and at $Q_0^2=1 \text{ GeV}^2$ it is about 180 GeV which corresponds to $x_{min} \approx 0.003$. Contribution

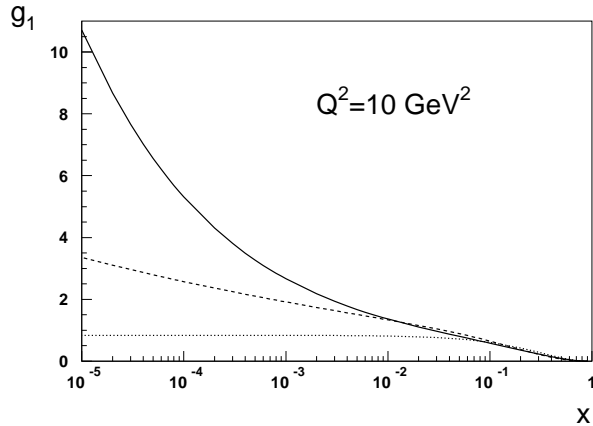


Figure 8: Non-singlet part of the proton spin structure function $g_1(x, Q^2)$ at $Q^2 = 10 \text{ GeV}^2$. Continuous line corresponds to full calculations, broken line is a pure leading order Altarelli–Parisi prediction, and a dotted one marks the nonperturbative input, $g_1^{(0)}$, assumed as $g_1^{(0)}(x) = 2g_A(1-x)^3/3$ and satisfying the Bjorken sum rule, $\Gamma_1 = g_A/6$. Figure taken from [20].

to the g_1 moments from the unmeasured region, $0 \leq x < 0.003$, has thus to be done phenomenologically.

Unified system of equations including the double $\ln^2(1/x)$ resummation effects and the complete leading-order Altarelli-Parisi evolution, [32], was used to extrapolate the spin dependent parton distributions and the polarised nucleon structure functions down to $x \sim 10^{-5}$, [36]. Calculated moments of the proton structure function for $2 < Q^2 < 15 \text{ GeV}^2$, i.e. where the low x measurements exist, agreed well with the latter and the estimated contribution of the integral over $g_1(x, Q^2)$ in the interval $10^{-5} < x < 10^{-3}$ was about 2% of the total g_1^p moment in the above interval of Q^2 . In the same limits of Q^2 , moments of g_1^n were found to lie below the experimental data and the calculated low x contribution was 8% of the total neutron moment. All these contributions increase with increasing Q^2 . It was also estimated that the above low x region contributes only in about 1% and 2% to the Bjorken and Ellis–Jaffe sum rules respectively.

Within the same formalism and at $Q^2=10 \text{ GeV}^2$, a contribution of 0.0080 from the unmeasured region, $0 \leq x < 0.003$, to the Bjorken integral was obtained while the contribution resulting from the pure LO Altarelli-Parisi evolution was 0.0057. These numbers have to be compared with 0.004 obtained when $g_1=\text{const}$ behaviour, consistent with Regge prediction was assumed and fitted to the lowest x data points for proton and deuteron targets (see [20] and references therein).

Extrapolation to the unmeasured region ($0 \leq x < 0.003$) of the NLO DGLAP fits to the world data results in about 10% contribution of that low x region to the g_1^p moment, [18]. The NLO DGLAP fit to the SMC data gave a contribution of 0.010 to the Bjorken integral at $Q^2=10$ GeV², i.e. about 6% of that integral, [18]. These numbers rely on the validity of the assumption that the parton distributions behave as x^δ as $x \rightarrow 0$.

5 Nonperturbative effects in g_1

Data on polarized nucleon structure function $g_1(x, Q^2)$ extend to the region of low values of Q^2 , [37, 8, 9, 12]. This region is of particular interest since nonperturbative mechanisms dominate the particle dynamics there and a transition from soft- to hard physics may be studied. In the fixed target experiments the low values of Q^2 are reached simultaneously with the low values of the Bjorken variable, x , cf. Figs 1 and 2, and therefore predictions for spin structure functions in both the low x and low Q^2 region are needed. Partonic contribution to g_1 which controls the structure function in the deep inelastic domain has thus to be suitably extended to the low Q^2 region and complemented by a non-perturbative component.

The low Q^2 spin-averaged electroproduction is very successfully described by the Generalised Vector Meson Dominance (GVMD) model, see e.g. [5, 6, 7]. Therefore methods based on GVMD should also be used to describe the behaviour of the g_1 in the low x , low Q^2 region. Two attempts using such methods have recently been made. In the first one, [35] the following representation of g_1 was assumed:

$$g_1(x, Q^2) = g_1^{VMD}(x, Q^2) + g_1^{part}(x, Q^2). \quad (7)$$

The partonic contribution, g_1^{part} which at low x is controlled by the logarithmic $\ln^2(1/x)$ terms, was parametrised as discussed in Section 4.2.

The VMD contribution, $g_1^{VMD}(x, Q^2)$, was represented as:

$$g_1^{VMD}(x, Q^2) = \frac{M\nu}{4\pi} \sum_{V=\rho,\omega,\phi} \frac{M_V^4 \Delta\sigma_V(W^2)}{\gamma_V^2(Q^2 + M_V^2)^2} \quad (8)$$

where M_V is the mass of the vector meson V , γ_V^2 are determined from the leptonic widths of the vector mesons and $\nu = Q^2/2Mx$. The unknown cross sections $\Delta\sigma_V(W^2)$ are combinations of the total cross sections for the scattering of polarised vector mesons and nucleons. It was assumed that they are proportional (with a proportionality coefficient C) to the appropriate combinations of the nonperturbative contributions $\Delta p_j^0(x)$

to the polarised quark and antiquark distributions:

$$\frac{M\nu}{4\pi} \sum_{V=\rho,\omega} \frac{M_V^4 \Delta\sigma_V}{\gamma_V^2 (Q^2 + M_V^2)^2} = C \left[\frac{4}{9} (\Delta u_{val}^0(x) + 2\Delta \bar{u}^0(x)) + \frac{1}{9} (\Delta d_{val}^0(x) + 2\Delta \bar{d}^0(x)) \right] \frac{M_\rho^4}{(Q^2 + M_\rho^2)^2}, \quad (9)$$

$$\frac{M\nu}{4\pi} \frac{M_\phi^4 \Delta\sigma_{\phi p}}{\gamma_\phi^2 (Q^2 + M_\phi^2)^2} = C \frac{2}{9} \Delta \bar{s}^0(x) \frac{M_\phi^4}{(Q^2 + M_\phi^2)^2}, \quad (10)$$

where $\Delta u^0(x) = \Delta p_u^0(x)$, etc. The $\Delta p_j^0(x)$, Eq.(5), behave as x^0 for $x \rightarrow 0$. As a result the cross sections $\Delta\sigma_V$ behave as $1/W^2$ at large W^2 which corresponds to zero intercepts of the appropriate Regge trajectories.

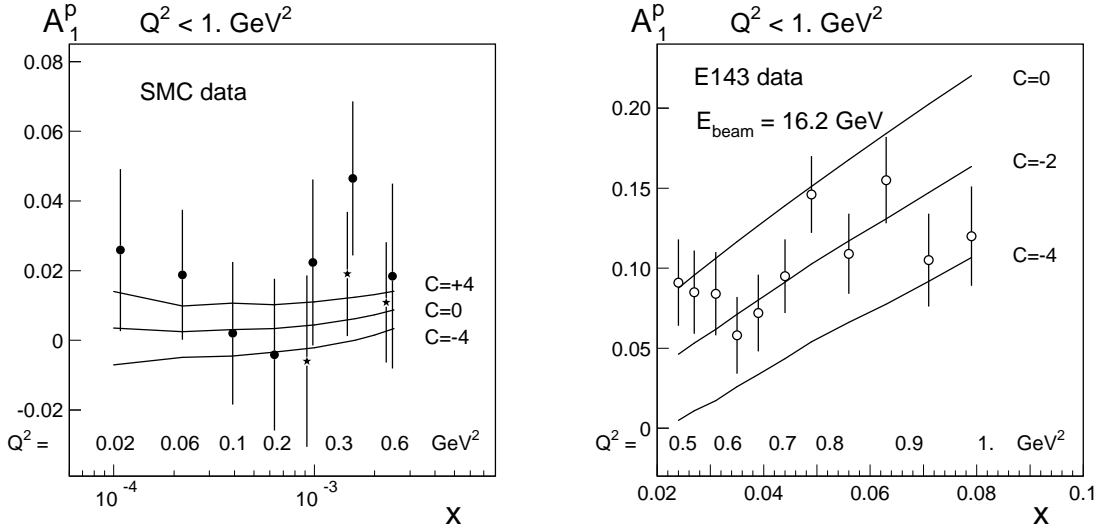


Figure 9: Spin asymmetry A_1 for the proton as a function of x at the measured Q^2 values (marked above the x axis), obtained by the SMC (stars [8] and dots [9]) and by SLAC E143 [37] (at 16.2 GeV incident energy only). Errors are statistical. Curves are predictions of the model for different values of C . Figure comes from [35].

Results of calculations for $Q^2 < 1 \text{ GeV}^2$ are shown in Fig.9 for different values of C . The statistical accuracy of the SMC data is too poor to constraint the value of the coefficient C . The SLAC E143 data apparently prefer a small negative value of C . Similar analysis of the neutron and deuteron spin structure functions was inconclusive.

In the other attempt to describe the $g_1(x, Q^2)$ in the low x , low Q^2 region, [38], the GVMD model was used together with the Drell-Hearn-Gerasimov-Hosoda-Yamamoto (DHGHY) sum rule, [39, 40, 41]. In the GVMD, the $g_1(x, Q^2)$ has the following representation, valid for fixed $W^2 \gg Q^2$, i.e. small values of x , $x = Q^2 / (Q^2 + W^2 - M^2)$:

$$g_1(x, Q^2) = g_1^L(x, Q^2) + g_1^H(x, Q^2) = \frac{M\nu}{4\pi} \sum_V \frac{M_V^4 \Delta\sigma_V(W^2)}{\gamma_V^2 (Q^2 + M_V^2)^2} + g_1^{AS}(\bar{x}, Q^2 + Q_0^2). \quad (11)$$

The first term sums up contributions from light vector mesons, $M_V < Q_0$ where $Q_0^2 \sim 1 \text{ GeV}^2$ [6]. The unknown $\Delta\sigma_V$ are expressed through the combinations of nonperturbative parton distributions, $\Delta p_j^0(x)$, evaluated at fixed Q_0^2 , similar to the previous case.

The second term in (11), $g_1^H(x, Q^2)$, which represents the contribution of heavy ($M_V > Q_0$) vector mesons to $g_1(x, Q^2)$ can also be treated as an extrapolation of the QCD improved parton model structure function, $g_1^{AS}(x, Q^2)$, to arbitrary values of Q^2 : $g_1^H(x, Q^2) = g_1^{AS}(\bar{x}, Q^2 + Q_0^2)$, cf. [7]. Here the scaling variable x is replaced by $\bar{x} = (Q^2 + Q_0^2)/(Q^2 + Q_0^2 + W^2 - M^2)$. It follows that $g_1^H(x, Q^2) \rightarrow g_1^{AS}(x, Q^2)$ as Q^2 is large. We thus get:

$$\begin{aligned} g_1(x, Q^2) &= C \left[\frac{4}{9}(\Delta u_{val}^0(x) + 2\Delta \bar{u}^0(x)) + \frac{1}{9}(\Delta d_{val}^0(x) + 2\Delta \bar{d}^0(x)) \right] \frac{M_\rho^4}{(Q^2 + M_\rho^2)^2} \\ &+ C \left[\frac{1}{9}(2\Delta \bar{s}^0(x)) \right] \frac{M_\phi^4}{(Q^2 + M_\phi^2)^2} \\ &+ g_1^{AS}(\bar{x}, Q^2 + Q_0^2). \end{aligned} \quad (12)$$

The only free parameter in (12) is the constant C . Its value may be fixed in the photoproduction limit where the first moment of $g_1(x, Q^2)$ is related to the anomalous magnetic moment of the nucleon via the DHGHY sum rule, cf. [42, 43]:

$$I(0) = I_{res}(0) + M \int_{\nu_t(0)}^{\infty} \frac{d\nu}{\nu^2} g_1(x(\nu), 0) = -\kappa_{p(n)}^2/4, \quad (13)$$

where the DHGHY moment before taking the $Q^2=0$ limit has been split into two parts, one corresponding to $W < W_t \sim 2 \text{ GeV}$ (baryonic resonances) and the other to $W > W_t$:

$$I(Q^2) = I_{res}(Q^2) + M \int_{\nu_t(Q^2)}^{\infty} \frac{d\nu}{\nu^2} g_1(x(\nu), Q^2). \quad (14)$$

Here $\nu_t(Q^2) = (W_t^2 + Q^2 - M^2)/2M$. Substituting $g_1(x(\nu), 0)$ in Eq. (13) by Eq. (12) at $Q^2 = 0$ we may obtain the value of C from (13) if $I_{res}(0)$, the contribution from resonances, is known e.g. from measurements.

To obtain the value of C from Eq. (13), $I_{res}(0)$ was evaluated using the preliminary data taken at ELSA/MAMI by the GDH Collaboration [44] at the photoproduction, for $W_t=1.8 \text{ GeV}$. The g_1^{AS} was parametrized using GRSV fit [22] for the ‘‘standard scenario’’ at the NLO accuracy. $Q_0^2 = 1.2 \text{ GeV}^2$ was assumed as in the analysis of F_2 , [6]. As a result the constant C was found to be -0.24 or -0.30 , for the $\Delta p_j^0(x)$ in Eq.(12) parametrised at $Q^2 = Q_0^2$ as Eq. (5) or as [22], respectively.

The nonperturbative, Vector Meson Dominance contribution was obtained negative in both attempts, [35, 38] as well as from earlier phenomenological analyses of the sum rules [43, 45].

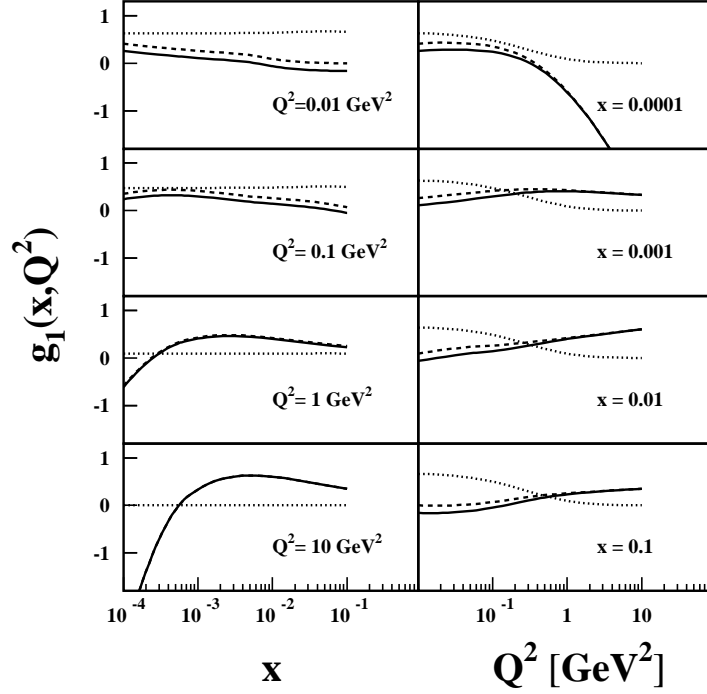


Figure 10: Values of xg_1 for the proton as a function of x and Q^2 , Eq.(12). The asymptotic contribution, g_1^{AS} , is marked with broken lines, the VMD part, g_1^L , with dotted lines and the continuous curves mark their sum, according to (12). Figure comes from [38].

The g_1 obtained from the above formalism is shown in Fig. 10. It reproduces well a general trend in the data, cf. Fig.11a; however experimental errors are too large for a more detailed analysis. To compute the DHGHY moment, Eq.(14), for the proton, preliminary results of the JLAB E91-023 experiment [46] for $0.15 \lesssim Q^2 \lesssim 1.2 \text{ GeV}^2$ and $W < W_t = W_t(Q^2)$ [47] were used. Results, Fig.11b, show that partons contribute significantly even at $Q^2 \rightarrow 0$ where the main part of the $I(Q^2)$ comes from resonances. The DHGHY moment is shown in Fig. 12 together with the results of calculations of Refs [45,48] as well as with the E91-023 measurements in the resonance region used as an input to the $I(Q^2)$ calculations. The E91-023 data corrected by their authors for the deep inelastic contribution are also presented. Results of calculations are slightly larger than the DIS-corrected data and the results of [45] but clearly lower than the results of [48] which overshoot the data.

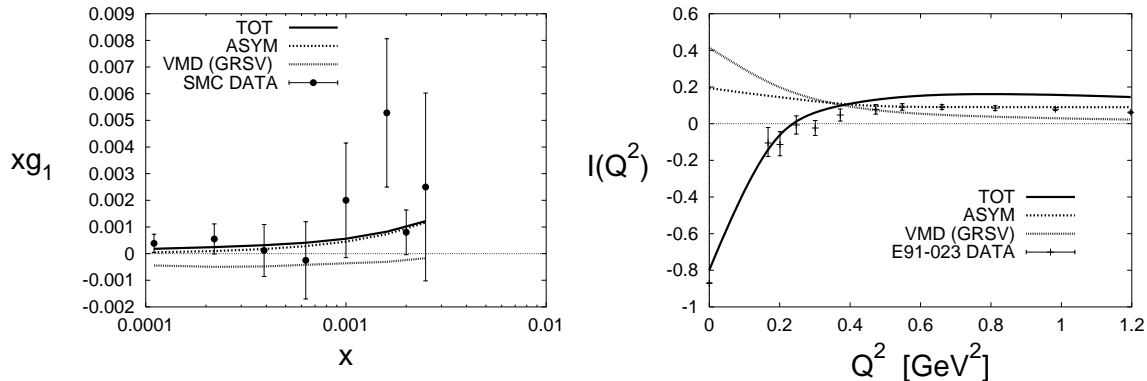


Figure 11: a) Values of xg_1 for the proton as a function of x at the measured values of Q^2 in the non-resonant region, $x < x_t = Q^2/2M\nu_t(Q^2)$. Both the VMD input and g_1^{AS} have been evaluated using the GRSV fit for standard scenario at the NLO accuracy [22]. Contributions of the VMD and of the xg_1^{AS} are shown separately. Points are the SMC measurements at $Q^2 < 1 \text{ GeV}^2$, [9]; errors are total. The curves have been calculated at the measured x and Q^2 values. b) The DHGHY moment $I(Q^2)$ for the proton. Details as in Fig.11a. Points mark the contribution of resonances as measured by the JLAB E91-023, [46] at $W < W_t(Q^2)$. Figures come from [38].

6 Outlook

The longitudinal spin dependent structure function, $g_1(x, Q^2)$, is presently the only observable which permits an insight into the spin dependent low x physics. Contrary to spin-independent structure functions, it is sensitive to double logarithmic, $\ln^2(1/x)$ corrections, generating its leading small x behaviour. However its knowledge is limited by the statistical accuracy and by the kinematics of the fixed-target experiments. In the latter, the low values of x are reached simultaneously with the low values of the four momentum transfer, Q^2 . While the low Q^2 domain may be of great interest due to a transition from soft to hard physics, it also challenges theoretical predictions based on partonic ideas which have to be suitably extended to the nonperturbative region.

Until now, experimental data on the $g_1(x, Q^2)$ at low x came mainly from the SMC at CERN. They do not permit to constrain the low x parton distributions, nor to test the Regge model but they seem to leave room for contributions other than (low Q^2 extrapolated) partonic mechanisms. They also permitted first quantitative studies of nonperturbative mechanisms; results consistently point towards large and negative contribution of the latter.

New low x data on $g_1(x, Q^2)$ will soon be available from COMPASS. Their statistics will be by far larger so that statistical errors should no longer be dominating. Also the

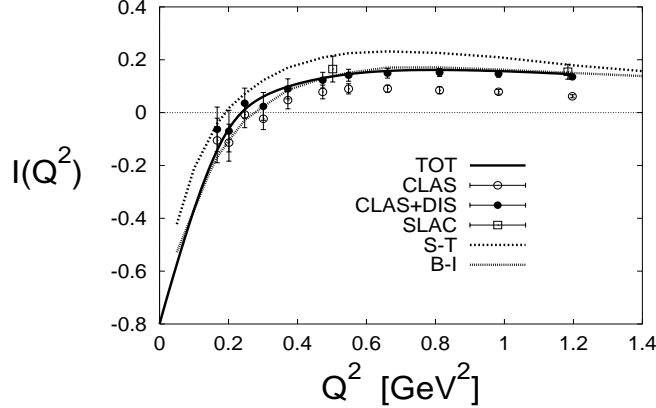


Figure 12: The DHGHY moment $I(Q^2)$ for the proton with the VMD part parametrized using the GRSV fit [22]. Shown are also calculations of [45] (“B–I”) and [48] (“S–T”). Points marked “CLAS” are from the JLAB E91-023 experiment [46]: the open circles refer to the resonance region, $W < W_t(Q^2)$ and the full circles contain a correction for the DIS contribution. Errors are total. Figure comes from [38].

experimental acceptance at low x will be much wider in the nonperturbative domain and thus tests of the Regge behaviour of g_1 will be possible. A crucial extension of the kinematic domain of the (deep) inelastic spin electroproduction will take place with the advent of the polarised Electron-Ion Collider, EIC, at BNL [49, 50]. With its centre-of-mass energy only about 2 times lower than that at HERA, this machine will open a field of perturbative low x spin physics where also other, semi-inclusive and exclusive observables, will be accessible for testing the high parton density mechanisms.

Acknowledgments

Many subjects in low x physics were for the first time addressed and developed by Jan Kwieciński. One of these is the non-perturbative aspect of the low x electroproduction. His involvement in the phenomenology of this exciting and still not understood branch of high energy physics was stimulated by the EMC measurements, followed by results of NMC, E665, SMC and HERA. I am greatly indebted to Jan for many years of most enjoyable scientific collaboration.

This research has been supported in part by the Polish Committee for Scientific Research with grant number 2P03B 05119.

References

- [1] A. Martin, in “Spin in physics”, X Séminaire Rhodanien de Physique, Villa Gualino, March 2002, edited by M. Anselmino, F. Mila and J. Soffer, Frontier Group.
- [2] J. Soffer, hep-ph/0212011, closing talk at the 15th International Spin Physics Symposium (SPIN2002), Long Island, NY, September 2002 (to appear in the Proceedings).
- [3] ZEUS Collaboration, S. Chekanov et al., Eur. Phys. J. **C21** (2001) 443; H1 Collaboration, C. Adloff et al., Phys. Lett. **B520** (2001) 183.
- [4] Small x Collaboration, B. Andersson et al., Eur. Phys. J. **C25** (2002) 77.
- [5] ZEUS Collaboration, J. Breitweg et al., Phys. Lett. **B487** (2000) 53 and references therein.
- [6] B. Badelek and J. Kwieciński, Z. Phys. **C43** (1989) 251.
- [7] B. Badelek and J. Kwieciński, Phys. Lett. **B295** (1992) 263.
- [8] SMC, B. Adeva et al., Phys. Rev. **D58** (1998) 112001.
- [9] SMC, B. Adeva et al., Phys. Rev. **D60** (1999) 072004 and erratum: *ibid.* **D62** (2000) 079902.
- [10] COMPASS Collaboration, C. Marchand, talk at the XIth International Workshop on Deep Inelastic Scattering (DIS2003), April 2003, St Petersburg, Russia; to appear in the Proceedings.
- [11] R. Windmolders, in “Spin in physics”, X Séminaire Rhodanien de Physique, Villa Gualino, March 2002, edited by M. Anselmino, F. Mila and J. Soffer, Frontier Group.
- [12] U. Stösslein, Proceedings of the Xth International Workshop on Deep Inelastic Scattering (DIS2002), May 2002, Cracow, Poland, Acta Phys. Pol. **B33** (2002) 2813.
- [13] R.L. Heimann, Nucl. Phys. **B64** (1973) 429; J. Ellis and M. Karliner, Phys. Lett. **B213** (1988) 73.
- [14] N. Bianchi and E. Thomas, Phys. Lett. **B450** (1999) 439.

- [15] F.E. Close and R.G. Roberts, Phys. Lett. **B336** (1994) 257.
- [16] S.D. Bass and P.V. Landshoff, Phys. Lett. **B336** (1994) 537.
- [17] J. Kuti in “The Spin Structure of the Nucleon”, World Scientific, Singapore, 1996; M.G. Ryskin, private communication (Durham, 1998).
- [18] SMC, B. Adeva et al., Phys. Rev. **D58** (1998) 112002.
- [19] A. De Roeck et al., Eur. Phys. J. **C6** (1999) 121.
- [20] B. Badelek and J. Kwieciński, Phys. Lett. **B418** (1998) 229.
- [21] For a review of early QCD analyses of g_1 see e.g. R. Windmolders, Nucl. Phys. B (Proc. Suppl.) **79** (1999) 51.
- [22] M. Glück, E. Reya, M. Stratmann and W. Vogelsang, Phys. Rev. **D63** (2001) 094005.
- [23] J. Blümlein and H. Böttcher, Nucl. Phys. **B636** (2002) 225.
- [24] E. Leader, A.V. Sidorov and D.B. Stamenov, Eur. Phys. J. **C23** (2002) 479.
- [25] C. Bourrely, J. Soffer and F. Buccella, Eur. Phys. J. **C23** (2002) 487.
- [26] E.A. Kuraev, L.N. Lipatov and V. Fadin, Zh. Eksp. Teor. Fiz. **72** (1977) 373 [Sov. Phys. JETP, **45** (1977) 199]; Ya. Ya. Balitzkii and L.N. Lipatov, Yad. Fiz. **28** (1978) 1597 [Sov. J. Nuc. Phys. **28** (1978) 822; L.N. Lipatov, in “Perturbative QCD”, edited by A.H. Mueller, World Scientific, 1989.
- [27] J. Bartels, B.I. Ermolaev and M.G. Ryskin, Z. Phys. **C70** (1996) 273; *ibid.* **C72** (1996) 627.
- [28] B.I. Ermolaev, S.I. Manayenkov and M.G. Ryskin, Z. Phys. **C69** (1996) 259; S.I. Manayenkov, Z. Phys. **C75** (1997) 685.
- [29] J. Kwieciński, Acta Phys. Pol. **B27** (1996) 893.
- [30] V.G. Gorshkov *et al.*, Yad. Fiz. **6** (1967) 129 (Sov. J. Nucl. Phys. **6** (1968) 95); L.N. Lipatov, Zh. Eksp. Teor. Fiz. **54** (1968) 1520 (Sov. Phys. JETP **27** (1968) 814. R. Kirschner and L.N. Lipatov, Nucl. Phys. **B213** (1983) 122; R. Kirschner, Z. Phys. **C67** (1995) 459.
- [31] J. Kwieciński, Phys. Rev. **D26** (1982) 3293.

- [32] J. Kwieciński and B. Ziaja, Phys. Rev. **D60** (1999) 054004.
- [33] J. Kwieciński, Acta Phys. Pol. **B29** (1998) 1201.
- [34] J. Blümlein and A. Vogt, Acta Phys. Polon. **B27** (1996) 1309; Phys.Lett. **B386** (1996) 350; J. Blümlein, S. Riemersma and A. Vogt Nucl. Phys. B (Proc. Suppl) **51C** (1996) 30.
- [35] B. Badełek, J. Kiryluk and J. Kwieciński, Phys. Rev. **D61** (2000) 014009.
- [36] B. Ziaja, Acta Phys. Pol., **B32** (2001) 2863.
- [37] SLAC, E143, K. Abe et al., Phys. Rev. **D58** (1998) 112003.
- [38] B. Badełek, J. Kwieciński and B. Ziaja, Eur. Phys. J. **C26** (2002) 45.
- [39] S.D. Drell and A.C. Hearn, Phys. Rev. Lett. **16** (1966) 908. 5A
- [40] S.B. Gerasimov, Sov. J. Nucl. Phys. **2** (1966) 430.
- [41] M. Hosoda and K. Yamamoto, Prog. Theor. Phys. Lett. **36** (1966) 425.
- [42] B.L. Ioffe, Surveys in High Energy Physics, **8** (1995) 107.
- [43] B.L. Ioffe, Phys. At. Nucl. **60** (1997) 1707.
- [44] GDH Collaboration, K. Helbing, Nucl. Phys. (Proc. Suppl.) **105** (2002) 113.
- [45] V. Burkert and B.L. Ioffe, Phys. Lett. **B296** (1992) 223; V. Burkert and B.L. Ioffe, J. Exp. Th. Phys. **78** (1994) 619.
- [46] JLAB E91-023, R. De Vita, talk at BARYONS 2002, Jefferson Lab., March 3-8, 2002, <http://www.jlab.org/baryons2002/program.html>.
- [47] JLAB E91-023, R. Fatemi, private communication (June 2002).
- [48] J. Soffer and O. Teryaev, Phys. Rev. Lett. **70** (1993) 3373.
- [49] See e.g. <http://www.bnl.gov/eic>.
- [50] S.D. Bass and A. De Roeck, Eur. Phys. J. **C18** (2001) 531.